A Retrospective Analysis of Spontaneous Sphenoid Sinus Fistula: MR and CT Findings

Prashant G. Shetty, Manu M. Shroff, Girish M. Fatterpekar, Dushyant V. Sahani, and Milind V. Kirtane

BACKGROUND AND PURPOSE: The sphenoid sinus is rarely implicated as a site of spontaneous CSF fistula. We undertook this study to evaluate the potential etiopathogenesis of spontaneous CSF fistula involving the sphenoid sinus and to review the imaging findings.

METHODS: We retrospectively reviewed the imaging findings of 145 cases of CSF fistula from our departmental archives (August 1995 through August 1998). Fifteen (10%) patients had CSF fistulas involving the sphenoid sinus. Eleven (7%) patients had spontaneous CSF fistulas, whereas in four patients, the CSF fistulas in the sphenoid sinus were related to trauma. Of the 11 patients, nine underwent only plain high-resolution CT and MR cisternography. One patient additionally underwent contrast-enhanced CT cisternography, and one other patient underwent MR cisternography only. For each patient, the CSF fistula site was surgically confirmed. The MR imaging technique included T1-weighted and fast spin-echo T2-weighted 3-mm-thick coronal sequences obtained with the patient in the supine position. The plain high-resolution CT study included 3-mm-thick, and sometimes 1- to 1.5-mm-thick, coronal sections obtained with the patient in the prone position. Similar sections were obtained after injecting nonionic contrast material intrathecally via lumbar puncture for the CT cisternographic study. We evaluated each of the 11 patients for the exact site of CSF leak in the sphenoid sinus. We also determined the presence of pneumatization of lateral recess of the sphenoid sinus, orientation of the lateral wall of the sphenoid sinus, presence of arachnoid pits, presence of brain tissue herniation, and presence of empty sella in each of these patients.

RESULTS: The exact sites of the CSF fistulas were documented for all 11 patients by using plain high-resolution CT, MR cisternography, or CT cisternography. In nine (82%) patients, the sites of the CSF fistulas were at the junction of the anterior portion of the lateral wall of the sphenoid sinus and the floor of the middle cranial fossa. In the remaining two (18%) patients, the sites of the CSF fistulas were along the midportion of the lateral wall of the sphenoid sinus. Of these 11 patients, one had bilateral sites of the CSF fistula at the junction of the anterior portion of the lateral wall of the sphenoid sinus with the floor of the middle cranial fossa. In nine (82%) patients, the presence of brain tissue herniation was revealed, and this finding was best shown by MR cisternography. Ten (91%) patients had extensive pneumatization of the lateral recess of the sphenoid sinus, with an equal number having outward concave orientation of the inferior portion of the lateral wall of the sphenoid sinus. In seven (63%) patients, the presence of arachnoid pits, predominantly along the anteromedial aspect of the middle cranial fossa, was shown. In seven (63%) patients, empty sella was shown. For comparison, we reviewed the CT studies of the paranasal sinuses in 100 age-matched control subjects from a normal population. Twenty-three had extensive lateral pneumatization of the sphenoid sinus along with outward concavity of the inferior portion of the lateral wall. None of these 23 patients had arachnoid pits.

CONCLUSION: The sphenoid sinus, when implicated as a site of spontaneous CSF leak, yields a multitude of imaging findings. These are extensive pneumatization of the lateral recess of the sphenoid sinus, outward concave orientation of the inferior portion of the lateral wall of the sphenoid sinus, arachnoid pits, and empty sella. Considering the normative data, we speculate that this constellation of findings could play a role in the etiopathogenesis of spontaneous sphenoid sinus fistulas. Our findings also show the efficacy of noninvasive imaging techniques, such as plain high-resolution CT and MR cisternography, in the evaluation of sphenoid sinus CSF leak. Our data also suggest that spontaneous sphenoid sinus CSF leak is not an uncommon occurrence.

A CSF fistula poses a diagnostic and therapeutic challenge to both the radiologist who must attempt to determine the site of the leak and the surgeon who must attempt to treat this lesion. Accurate lo-
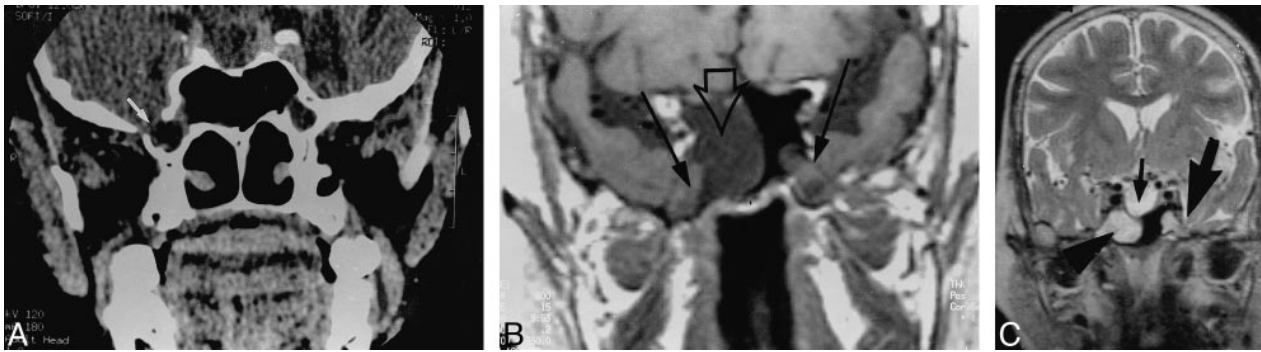
FIG 1.   Patient 11.
   A, Coronal high-resolution CT scan, obtained through the sphenoid sinus, shows a defect at the junction of the anterior portion of the lateral wall of the sphenoid sinus on the right side with the floor of the middle cranial fossa (*arrow*) associated with a meningocele. Note the concave lateral wall on the right side. CSF is seen on both sides of the sphenoid sinuses.
   B, Coronal T1-weighted (600/15/2) MR image of the brain clearly depicts brain tissue herniating through the bony defects bilaterally (*long arrows*). The *open arrow* points to the CSF in the right sphenoid sinus.
   C, Coronal T2-weighted (4600/90/2) MR image of the brain shows herniation of brain tissue (*thick arrow*) and CSF (*arrowhead*) bilaterally. Empty sella is also seen (*small arrow*).

calization of CSF fistulas not only makes the planning of surgery easier but also increases the chances of successful dural repair and decreases the possibility of negative exploration. This is especially true in this era of nasal endoscopic surgery in which the field of view is limited and accurate localization is therefore imperative.

   The most common site of CSF leakage is through the floor of the anterior cranial fossa, which communicates with the ethmoid or frontal sinuses or with the nasal fossa. The sphenoid sinus is rarely implicated as a source of spontaneous CSF fistula (1). Trauma is cited as the most common cause of CSF fistulas, although spontaneous CSF leakage is also known to occur. The purposes of this study were to evaluate the etiopathogenesis of spontaneous CSF fistula involving the sphenoid sinus and to correlate it with the imaging findings.

Methods

   We retrospectively reviewed the sites of spontaneous CSF fistulas that occurred in 11 patients in whom the sphenoid sinus was implicated as the site of leak. Plain high-resolution CT, MR cisternography, CT cisternography, or a combination of these techniques were used to identify the exact sites of the CSF fistulas, all of which were surgically confirmed.

   The CT protocol was conducted using Hi Speed CT/i. For the plain high-resolution CT study, 3-mm-thick coronal CT scans were obtained through the anterior cranial fossa and sphenoid sinus with the patient in the prone position. One- to 1.5-mm-thick contiguous sections were obtained through the region of interest for greater bone detail. A field of view of 120 mm and a matrix size of 512×512 were used. A bone algorithm was used to enhance bone detail. MR cisternography was performed using a 1.5-T Magnetom SP 6000. A coronal fast spin-echo T2-weighted MR sequence was obtained with parameters of 6000/90/1 (TR/TE/excitations), a section thickness of 3 mm, a distance factor of 0.1, a field of view of 230 mm, and a matrix of 192×256. T1-weighted coronal sequences with parameters of 600/12/3 were obtained in a similar manner. The patients underwent scanning in the supine position because they found it uncomfortable to lie in the prone position in the head coil.

   For CT cisternography, 8 mL of nonionic contrast material (180 mg I/mL) was injected intrathecally via lumbar puncture. The patient was then placed in the prone position, with the head at low position to allow the contrast material to enter the intracranial subarachnoid space. Three-millimeter-thick coronal scans were obtained through the anterior cranial fossa and roof of the sphenoid sinus with the patient in the prone position. One- to 1.5-mm-thick contiguous coronal scans were obtained through the region of interest for better definition of the CSF leak. A field of view of 120 mm and a matrix size of 512×512 were used with a bone algorithm for better definition of the CSF leak.

   We reviewed the 11 patients with spontaneous CSF fistulas involving the sphenoid sinus. We sought to determine the exact sites of the CSF fistulas in the sphenoid sinus. We also attempted to confirm the fistula-associated presence or absence of brain tissue herniation and pneumatized lateral recess of the sphenoid sinus. We identified the orientation of the lateral wall of the sphenoid sinus of the involved side, presence or absence of the arachnoid pits or holes, associated presence or absence of empty sella, and ventricular size.

   The patients ranged in age from 36 to 70 years. There were seven female and four male patients. All of the patients had spontaneous CSF fistulas. The imaging criteria for CSF fistula included a bone defect with CSF column communicating from the subarachnoid space extracranially or herniation of brain tissue/meninges extracranially or both. Nine patients underwent plain high-resolution CT and MR cisternography. One patient (patient 10) also underwent contrast-enhanced CT cisternography, and one other patient underwent MR cisternography only.

Results

   In nine (82%) patients, the site of the CSF fistulas was at the junction of the anterior portion of the lateral wall of the sphenoid sinus and the floor of the middle cranial fossa (Fig 1A). Brain tissue herniation was revealed in an equal number of patients and was best shown by MR cisternography (Fig 1B). One patient who had undergone CT cisternography had brain tissue herniation revealed at surgery. One patient (patient 11) had bilateral sites of a CSF fistula, although she clinically presented with a right-sided CSF rhinorrhea (Fig 1B).
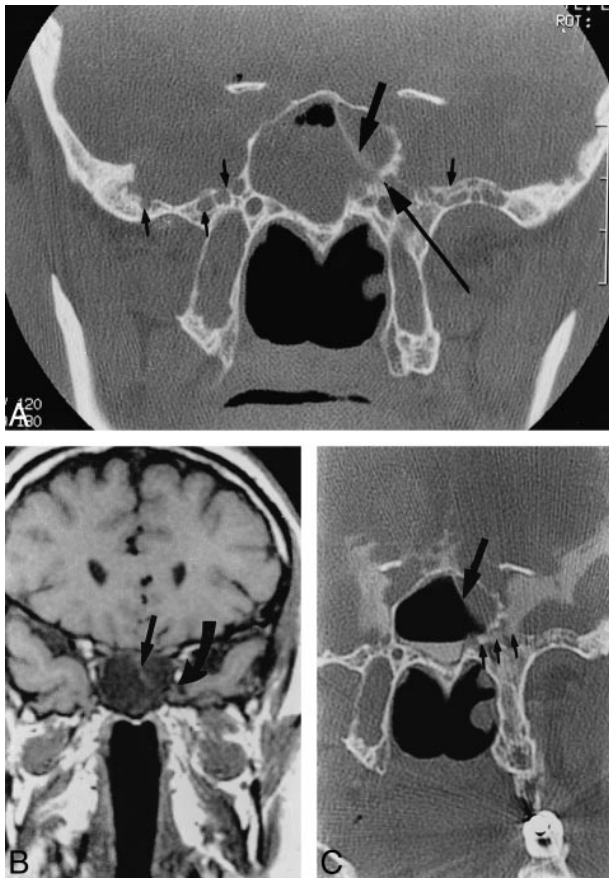
FIG 2. Patient 10.

A, Coronal high-resolution CT scan, obtained through the sphenoid sinus, shows a defective intersphenoid septum deviated to the left (*thick arrow*). The *long arrow* points to the defect in the anterior portion of the lateral wall of the sphenoid sinus on the left side, just inferior to the attachment of the septum. The *small arrows* depict arachnoid pits.

B, Coronal T1-weighted (600/15/2) MR image of the brain shows brain tissue herniating through the defect (*curved arrow*) in the anterior portion of the lateral wall of the sphenoid sinus on the left side. The *straight arrow* shows the defective intersphenoid septum.

C, CT cisternography scan shows the CSF tracking through the defect in the anterior portion of the lateral wall of the left sphenoid sinus into the right side (*small arrows*). The defective intersphenoid septum (*thick arrow*) is seen inserted just superior to this defect.
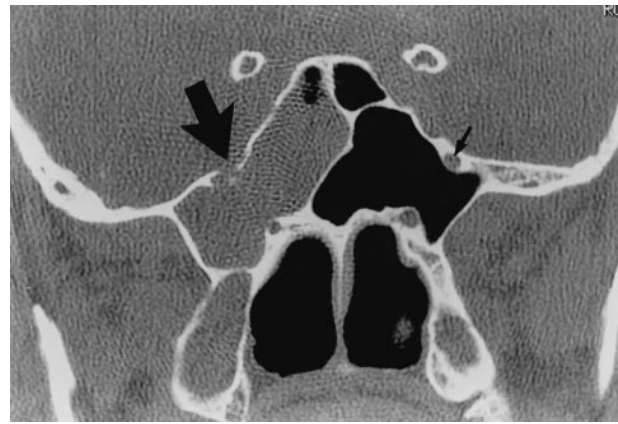

FIG 3. Patient 5. Coronal high-resolution CT scan, obtained through the sphenoid sinus, shows the presence of a defect in the lateral wall of the sphenoid sinus on the right side through the region of the foramen rotundum (*large arrow*). The *small arrow* points to the normal foramen on the left.

Plain high-resolution CT was useful in the identification of CSF fistulas in all 10 patients (11 sites of CSF fistulae) in whom this study was undertaken. One patient underwent MR cisternography only.

Ten (91%) patients had extensive pneumatization of the sphenoid sinus with lateral extensions (recesses). In all 10 patients, the involved lateral walls had an outward concave orientation inferiorly. In one patient (patient 3), the sphenoid sinus did not have lateral pneumatization and an outward convex orientation of the lateral wall of the sphenoid sinus was observed.

The presence of point erosions (arachnoid pits) along the anteromedial aspect of the middle cranial fossa was revealed in seven (63%) patients. An empty sella was revealed in seven (63%) patients. None of these patients had clinical signs of raised intracranial pressure. None of these patients had increased ventricular size. The surgeons confirmed the site of CSF leakage at the time of surgery, correlating their findings with those of the imaging study. We reviewed the CT studies of the paranasal sinuses in 100 age-matched control subjects from the normal population. Twenty-three had extensive lateral pneumatization of the sphenoid sinus along with outward concavity of the inferior portion of the lateral wall. None of these 23 patients had arachnoid pits. The results are presented in the Table.

Although imaging revealed a right-sided CSF rhinorrhea in patient 10, the site of CSF fistula was identified to be at the junction of the anterior aspect of the lateral wall of the sphenoid sinus, with the floor of the middle cranial fossa on the left side. The right-sided CSF rhinorrhea may have been caused by the orientation of the intersphenoid septum, which was proved by endoscopic surgery (Fig 2A and B).

In the remaining two patients, the CSF fistulas were located along the lateral wall of the sphenoid sinus (Fig 3). The floor of the sella was intact in each of these patients. In seven patients, the CSF fistulas were on the left side. The CSF fistulas were revealed to be on the right side in three patients. One patient (patient 11) had a bilateral CSF fistula.

Discussion

Precise anatomic localization of a CSF fistula helps in surgical planning and enhances the chance of successful dural repair, thereby decreasing the number of recurrent explorations. Usually, anterior cranial fossa leaks are tackled successfully via nasal endoscopic surgery. The surgical treatment of CSF fistulas involving the lateral recess of the sphenoidal sinus differs from the surgical strategy

Case summary of patients with spontaneous sphenoid sinus fistula

Patient No.	Age(yrs) /Sex	Side	Site	Brain Herniation	Pneumatised Lateral Wall of Sphenoid Sinus	Orientation of Lateral Wall of Sphenoid Sinus	Arachnoid Pits	Empty Sella	Additional Comments
1	37/M	Left	Junction of lateral wall of sphenoid sinus with floor of middle cranial fossa	+	+	Outwardly concave	−		No hydrocephalus
2	56/F	Right	Junction of lateral wall of sphenoid sinus with floor of middle cranial fossa	+	+	Outwardly concave	+	+	No hydrocephalus
3	68/M	Left	Junction of lateral wall of sphenoid sinus with floor of middle cranial fossa	+	−	Outwarldy convex	−	+	No hydrocephalus
4	50/F	Left	Junction of lateral wall of sphenoid sinus with floor of middle cranial fossa	+	+	Outwardly concave	+		No hydrocephalus
5	55/F	Right	Along mid lateral wall of sphenoid sinus	+	+	Outwardly concave	−	−	No hydrocephalus Fistula site involved foramen rotundum
6	45/M	Left	Junction of lateral wall of sphenoid sinus with floor of middle cranial fossa	+	+	Outwardly concave	−	+	No hydrocephalus
7	57/F	Left	Junction of lateral wall of sphenoid sinus with floor of middle cranial fossa	−	+	Outwardly concave	+	+	No hydrocephalus
8	38/F	Left	Along mid lateral wall of sphenoid sinus	+	+	Outwardly concave	+	+	No hydrocephalus
9	36/F	Right	Junction of lateral wall of sphenoid sinus with floor of middle cranial fossa	+	+	Outwardly concave	+	−	No hydrocephalus
10	44/M	Left	Junction of lateral wall of sphenoid sinus with floor of middle cranial fossa	−	+	Outwardly concave	+	+	Defective orientation of the inter sphenoid septum allowed fluid to cross over from the left to the right sphenoid sinus
11	70/F	Right	Junction of lateral wall of sphenoid sinus with floor of middle cranial fossa (bilateral)	+ (bilateral)	+	+	+	+	Bilateral meningoencepaloceles. The dura arachnoid complex had given way to CSF leakage on the right side while it was intact on the left.

for more medial sphenoidal fistulas. Fistulas involving a lateral extension of the sphenoid sinus require a transcranial approach for direct visualization and obliteration of the defect, whereas fistulas involving the central portion of the sinus may be successfully obliterated across the sphenoid (1, 2). Although it seems reasonable to pack the sphenoid sinus with fat, fascia, or fibrin glue for a CSF fistula involving the central portion of the sphenoid sinus, it would be easier to obliterate the laterally placed defect under endoscopic visualization. Nonetheless, minimally invasive nasal endoscopic surgery seems to be promising for the repair of both types of sphenoid sinus CSF fistulas (1, 3).

The most common site of CSF fistulas is at the floor of the anterior cranial fossa (2). Less commonly, the sphenoid sinus and the petrous temporal bone are implicated as CSF fistula sites (5). The sphenoid sinus is prone to CSF leakage, particularly when anatomic variants predispose it to develop

a communication with the sellar floor or the middle cranial fossa. Communication with the middle cranial fossa is the more likely if the sphenoid sinus is laterally pneumatized and is associated with arachnoid pits along its anteromedial aspect.

The junction of the lateral wall of the sphenoid sinus and the floor of the middle cranial fossa is perhaps the weakest site structurally and results in an anteromedial temporal encephalocele, one of the five major categories of temporal encephaloceles (4). In our series, all 11 patients had CSF fistulas involving the lateral wall of the sphenoid sinus. In nine (82%) patients, the CSF fistula site was at the junction of the anterior portion of the lateral wall of the sphenoid sinus and the floor of middle cranial fossa. In the remaining two patients, the fistula site was located in the midportion of the lateral wall of the sphenoid sinus. The sellar floor was intact in all patients.

A wide range in the degree of pneumatization of the sphenoid sinus exists, as shown by anatomic studies (7). Cope (8) found a clearly marked lateral recess in 72 (25%) of 292 sphenoid bones examined, with some of the recesses extending as far as the foramen rotundum. Rarely, the extension was seen to involve the pterygoid process (9). We also reviewed plain CT studies of the paranasal sinuses in 100 age-matched control subjects from the normal population. Twenty-three had extensive lateral pneumatization of the sphenoid sinus. All of these 23 patients also had outward concavity of the inferior portion of the lateral wall. Nevertheless, none of the 100 patients had arachnoid pits. Six of the patients had empty sella, but these patients did not have laterally pneumatized sphenoid sinuses. In our series, the presence of extensive pneumatization of the lateral wall of the sphenoid sinus was noted in 10 (91%) patients. The pneumatization of the pterygoid plate results in lateral extension of the sphenoid sinus beyond the body of the sphenoid bone. This may well be the cause of the oblique orientation of the lateral wall of the sphenoid sinus. We speculate that the vector forces of CSF pulsations act along the anteromedial aspect of the middle cranial fossa, resulting in an outward concave orientation of the lateral wall of the sphenoid sinus. This is supported by the concave orientation of the lateral wall found in 10 (91%) patients in this series. It has also been hypothesized that the CSF pressures and the hydrostatic pulsatile forces may lead to the development of small holes or pits at the sites of arachnoid villi with herniation of dura/arachnoid or brain tissue (10−13). With fixation of these meninges in the pits, the dura mater progressively thins out, resulting in fenestration, arachnoid diverticula formation, or CSF fistula when the arachnoid membrane ruptures. The findings of pits or irregularity along the floor of the middle cranial fossa were seen in seven (63%) patients in our series. Russell (10) postulated that intermittently raised intracranial pressure from straining and coughing and possibly rupture of the arachnoid membrane could cause thinning in the bone and dura mater. O'Connell (14) suggested that periods of hypoxia could cause alterations in the CSF pressure, contributing to a similar effect.

Secondary pneumatization (ie, pneumatization of the sphenoid wings) does not start until the age of 10 years. The fact that none of our patients were children further corroborates the relevance of the lateral recesses in cases of spontaneous CSF fistula.

Primary empty sella syndrome is caused by a combination of congenitally deficient diaphragmatic sella and chronically elevated CSF pressure (15−17). Spontaneous CSF rhinorrhea is a recognized sequela to primary empty sella (18). Davis and Kaye (19), in a landmark article, presented a case of primary empty sella syndrome with spontaneous CSF rhinorrhea, in which the use of continuous intracranial pressure monitoring revealed a high baseline pressure with intermittent peaks. The highlighting feature of this article was not only the hitherto undocumented proof of the relationship of empty sella syndrome and raised intracranial pressure but also the cessation of CSF leak after a lumboperitoneal shunt. Primary empty sella was documented to exist in seven patients in our series. None of the patients, however, showed evidence of CSF leak from the sellar floor. All leaks involved the lateral wall of the sphenoid sinus. We speculate that the inherent weakness in the lateral wall caused by lateral pneumatization of the sphenoid sinus, perhaps compounded by the altered CSF dynamics, resulted in the lateral wall's giving way, resulting in CSF fistula. Empty sella syndrome is known to occur predominantly in the female population (18). We observed this finding in seven (63%) patients in our series. Partial empty sella was observed in three patients.

For patient 11, who presented with right-sided CSF fistula, MR cisternography and high-resolution CT revealed bone defects at the junction of the lateral wall of the sphenoid sinus and the floor bilaterally associated with meningoencephaloceles. Although the dura-arachnoid complex had given way to CSF leakage on the right side, it was intact on the left (no CSF leakage on the left) (Fig 1).

Patient 10 presented with a right-sided CSF fistula. CT cisternography performed elsewhere revealed extreme thinning of the anteromedial aspect of the middle cranial fossa on the left side caused by extensive arachnoidal pits. Because of the orientation of the intersphenoidal septum, the CSF leakage presented clinically on the right side, although the fistula site was on the left. CT cisternography definitely added to our confidence in diagnosing the exact fistula site in this patient (Fig 2A). In our case series, however, in only one patient (patient 5) was the site of CSF leak through the region of the foramen rotundum shown (Fig 3).

An interesting clinical feature was increased CSF egression when seven of our patients bent forward. This could be related to the relationship of the sphenoid ostium to the sinus floor. The sphenoid

ostium lies at an appreciable distance anterosuperior from the sinus floor. An increase in the CSF rhinorrhea therefore occurs in a case of sphenoid sinus leak when the patient bends forward as an increasing amount of CSF gains access to the ostium "teapot" sign.

Plain high-resolution CT offers superb bone detail and can give indirect evidence of a CSF fistula by revealing a bone defect and opacification of sinuses or air cells. MR cisternography can noninvasively reveal CSF leakage in multiple planes without the disadvantage of ionizing radiation. On the T2-weighted fast spin-echo sequence, the bright signal emanating from the CSF column is well visualized against the paranasal sinuses' background of air (20). The CSF fistula is better visualized using 1-mm-thick sections through the suspected site of CSF leakage. Close monitoring of the study by an experienced radiologist is important to obtain thin sections through the region of interest to document the exact site of CSF fistula. MR cisternography is useful in showing the presence of brain tissue/meningeal herniation. Compared with CT, herniated brain tissue is better shown by MR cisternography. This may be partly because of better soft-tissue resolution of MR cisternography, but a remote possibility is that the prone position used during CT might cause an alteration in the magnitude of brain tissue.

Nasal endoscopic surgery is increasingly being used over the conventional intracranial approach. Therefore, the interpreting neuroradiologist's role in showing the exact site of the leak is essential. The neuroradiologist has the information to forewarn the surgeon regarding the presence of a dehiscent optic nerve or internal carotid artery and the presence of brain tissue herniation, especially because a limited field of view is available to the surgeon who is performing the endoscopic surgery. Detailing the above information not only makes the surgical planning smoother but also prevents a surgical catastrophe.

Conclusion

Twenty-three of 100 age-matched control subjects showed lateral pneumatization of the sphenoid sinus as opposed to 91% of the patients in this series. None of the age-matched controls had arachnoid pits, whereas 63% of the patients in this series had this finding. We therefore speculate that the combination of laterally pneumatized sphenoid si-

nus with arachnoid pits at the floor of the middle cranial fossa makes this site most susceptible to CSF leakage. Plain high-resolution CT and MR cisternography can noninvasively reveal the source of CSF fistula in these patients.

References

1. Landrenean FE, Mickey B, Coimbra C. **Surgical treatment of cerebrospinal fluid fistula involving lateral extension of the sphenoid sinus.** *Neurosurgery* 1998;42:1101–1105
2. Komisar A, Weitz S, Ruben RJ. **Rhinorrhea and pneumocephalus after cerebrospinal fluid shunting: the role of lateral extensions of the sphenoid sinus otolaryngol.** *Head Neck Surg* 1986;94:194–197
3. Dodson FE, Gross CW, Swerdloff JL, Gustafson LM. **Transnasal endoscopic repair of cerebrospinal fluid rhinorrhea and skull base defects: a review of twenty-nine cases.** *Otolaryngol Head Neck Surg* 1994;111:600–605
4. Benedict M, Schultz-Coulon HJ. **Spontaneous cerebrospinal rhinorrhea.** *HNO* 1991;39:1–7
5. Yeates AE, Blumenkopf B, Drayer BP, Wilkins R H, Osbourne S, Heinz ER. **Spontaneous CSF rhinorrhea arising from middle cranial fossa: CT demonstration.** *AJNR Am J Neuroradiol* 1984;5:820–821
6. Kumar R, Jenkins A. **Spontaneous CSF rhinorrhoea due to temporosphenoidal encephalocele.** *Br J Neurosurg* 1998;12:66–68
7. Christie M. **Cerebrospinal fluid fistula involving the sphenoid sinus.** *Neurosurgery* 1987;20:1
8. Cope VZ. **The internal structures of the sphenoid sinus.** *J Anat* 1961;51:127–136
9. Peele JC. **Unusual anatomical variations of the sphenoid sinus.** *Laryngoscope* 1957;67:208–237
10. Russell DS. *Observation on the Pathology of Hydrocephalus: Medical Research Council Special Report 265.* 4th impression. London: Her Majesty's Stationery Office; 1968:117–119
11. Wolbach SB. **Multiple hernias of the cerebrum and the cerebellum, due to intracranial pressure.** *J Med Res* 1908;19:153–173
12. Morris H. *Morris' Human Anatomy.* Schaeffer JP, ed. 10th ed. Philadelphia: Blakiston; 1942:1376
13. Kaufman B, Nulsen FE, Weiss MH, et al. **Acquired spontaneous, non-traumatic normal pressure cerebrospinal fluid fistula originating from the middle cranial fossa.** *Radiology* 1977;122:379–387
14. O'Connell JEA. **The vascular factor in intracranial pressure and maintenance of cerebrospinal fluid circulation.** *Brain* 1943;66:204–228
15. Kaufman B. **The "empty" sella turcica a manifestation of the intrasellar subarachnoid space.** *Radiology* 1968;90:931–941
16. Foley KM, Posner JM. **Does pseudotumor cerebri cause empty sella syndrome?** *Neurology* 1975;25:565–569
17. Neelon FA, Goree JA, Lebovitz HE. **The primary empty sella: clinical and radiographic characteristics and endocrine functions.** *Medicine* 1973;52:73–92
18. Jordan RM, Kendall JW, Kerker CW. **The primary empty sella syndrome: analysis of the clinical characteristics, radiographic features, pituitary functions and cerebrospinal fluid adenohypophysial hormone concentration.** *Am J Med* 1968;31:214–225
19. Davis S, Kaye AH. **A dynamic pressure study of spontaneous CSF rhinorrhea in the empty sella syndrome.** *J Neurosurg* 1980;52:103–105
20. Shetty PG, Shroff MM, Sahani DV, Kirtane MV. **Evaluation of high resolution CT and MR cisternography in the diagnosis of cerebrospinal fluid fistula.** *AJNR Am J Neuroradiol* 1998;19:633–639